Journal of Neuroinflammation

RESEARCH

Open Access

# Regulatory T cell expansion prevents retinal degeneration in type 2 diabetes

María Llorián-Salvador[1,2*], Daniel Pérez-Martínez[2], Miao Tang[3], Anna Duarri[4], Marta García-Ramirez[2,5], Anna Deàs-Just[2], Anna Álvarez-Guaita[2], Lorena Ramos-Pérez[2,5], Patricia Bogdanov[2,5], Jose A. Gomez-Sanchez[6,7], Alan W. Stitt[8], Cristina Hernández[2,5], Alerie G. de la Fuente[6,7] and Rafael Simó[2,5*]

## Abstract

**Background** The global incidence of type 2 diabetes (T2D) is rapidly increasing, with retinopathy being its most common complication and a leading cause of preventable blindness. Although the precise mechanisms involved in the development of diabetic retinopathy (DR) are not fully understood, defective immunomodulation is a recognized key factor in its pathophysiology. Regulatory T cells (Treg) regulate inflammation and promote regeneration, and while they are known to have important anti-inflammatory and neuroprotective roles in other tissues, including central nervous system, their role in the diabetic retina remains largely unknown. The aim of the present study is to examine the effect of Treg expansion of retinal neurodegeneration, an early event in the pathogenesis of DR.

**Methods** Treg expansion was achieved by co-injecting recombinant mouse IL-2 with anti-IL-2 monoclonal antibody or its isotype in db/db mice as an established model of T2D. Treg expansion was confirmed via flow cytometry in blood, spleen, and retina. Fundus angiography was performed in the days prior to animal sacrifice at 18 weeks. To study the effect of Tregs on retinal neurons, glia and vascular permeability, immunohistochemistry against Cone-Arrestin, PKCα, synaptophysin, ChAT, TH, GFAP, Iba-1, calbindin, Brn3a, RBPMS, isolectin B4, and albumin was used. Retinal VEGF levels were measured with a magnetic bead-based immunoassay, and NLRP3, Casp1, p20 and IL-18 were analyzed by Western Blot in retinal homogenates.

**Results** There was a significant decrease in Treg in db/db mice blood. When this deficiency was corrected in db/db mice by systemic Treg expansion, there was an effective protection against retinal neurodegenerative, gliotic, inflammatory changes and vascular leakage associated with T2D. Importantly, Treg expansion did not impact the T2D phenotype in db/db mice as evaluated by blood glucose, HbA1c and circulating insulin.

**Conclusion** Treg modulation in T2D offers a promising therapeutic approach to prevent early stages of DR. This strategy focuses on reducing neuroinflammation and mitigating the associated neuronal, glial, and vascular degenerative changes characteristic of DR.

**Keywords** Regulatory T cells, Diabetic retinopathy, Immunomodulation, Retina, Neurodegeneration, Inflammation, Type 2 diabetes

*Correspondence:
María Llorián-Salvador
maria.llorian@vhir.org
Rafael Simó
Rafael.simo@vhir.org

Full list of author information is available at the end of the article

## Introduction

T2D is one of the most common metabolic diseases in western societies and it is considered "the epidemic of the 21st century": affecting 1 in 11 people in Europe [1]. DR is a common T2D complication and the leading cause of preventable visual impairment in the working-age population [2], accounting for 15–17% of total blindness in Europe [3]. Current DR treatments, such as laser photocoagulation, intravitreal injections of corticosteroids or anti-vascular endothelial growth factor (VEGF) agents, are focused on the late-stages of the disease. Besides, IV agents have shown limited efficacy, significant risk of side-effects and they are very expensive. Therefore, new and more effective therapeutic strategies that limit the escalation of DR from its early stages and thereby prevent blindness and its associated social and economic burden, are an urgent need for the global healthcare.

DR is currently considered a highly specific neurovascular disease rather than merely a microvascular disease [4]. From a pathophysiological point of view, special emphasis has been placed on the retinal Neurovascular Unit (NVU) [5], which consists of vascular elements, basement membrane, neurons, glial cells (Müller glia, astrocytes) and immune cells such as microglia and perivascular macrophages. It is widely accepted that chronic inflammation is the main common pathogenic driver in the natural course of T2D [6] and its complications, including DR [7–9]. Chronic low-grade inflammation leads to a maladaptive innate immune system, contributing to DR development via infiltration of circulating immune cells and serum proteins into the retina [8–10]. This immune infiltration drives localized retinal inflammation mediated by microglia, Müller cells and endothelial cells, which in turn leads to NVU damage and subsequent neurodegeneration [7, 8, 11]. Glial cell activation and the subsequent release of pro-inflammatory and apoptotic cytokines and angiogenic factors is one of the most important underlying mechanisms of this prolonged neuroinflammation, which exacerbates oxidative stress and retinal neurovascular damage [7, 12].

Treg are a key component of the adaptive immune system and play a vital role in immune tolerance due to their potent immunosuppressive properties [13–15]. Treg migrate into tissues and dampen inflammation, suppressing other adaptive or innate immune cells [14]. In recent years, new functions of Treg beyond their immune regulatory properties have been discovered, with a growing evidence for Treg regenerative and neuroprotective functions in various tissues, including the central nervous system (CNS). Treg promote remyelination in models of multiple sclerosis (MS) [16], while in Alzheimer's disease (AD) and Parkinson's disease (PD), Treg restore homeostasis and prevent cognitive decline (CD) by eliminating neuroimmunogens, polarising microglia, modulating astrocytes and restoring normal neuronal function [13, 15]. Furthermore, the enhancement of astrocyte-mediated interleukin (IL)-2 production to locally expand Treg numbers in the CNS prevents inflammatory damage and facilitates repair following traumatic brain injury and age-associated CD [17, 18].

Given these neuroprotective, pro-regenerative and immunomodulatory roles, the beneficial effects of Treg expansion are currently under investigation in numerous clinical trials for AD, PD or MS [15, 19]. Since immunomodulation plays a significant role in the pathogenesis of DR it is plausible that Treg expansion may also be beneficial in this neurodegenerative disease [7–9].

Here, we provide experimental evidence that Treg expansion in early T2D rescues T2D-associated retinal pathology, preventing retinal neurodegeneration and reactive gliosis and reducing inflammasome activation. Our findings demonstrate that the well-established immunomodulatory role of Treg can be harnessed to prevent early-stage damage in DR and may and may help slow or prevent neurodegeneration, representing a new therapeutic strategy for treating this devastating complication of T2D.

## Materials and methods

### Animals

Diabetic male db/db (BKS.Cg-Dock7m +/+ Leprdb/J) mice and their control, non-diabetic mice (db/+; (BKS.Cg-Dock7m+Leprdb/+) were acquired from Charles River Laboratories (Calco, Italy) at 6 weeks of age. The mutated leptin receptor carried by db/db mice gave rise to an obesity-induced type 2 diabetes phenotype. Mice were bred and maintained in the animal facilities of the Vall d'Hebrón Research Institute (VHIR). With the aim of minimizing variability, mice were randomly distributed (block randomization) into groups of two mice per cage in Tecniplast GM-500 cages (36 cm × 19 cm × 13.5 cm) under standard laboratory conditions at 22±2 °C, with relative humidity of 50–60% and cycles of 12 h light/darkness. The cages were equipped with nesting material, absorbent bedding (BioFresh Performance Bedding 1/800 Pelleted Cellulose, Absorption Corp, Ferndale, WA, USA), ad libitum food (ENVIGO Global Diet Complete Feed for Rodents, Mucedola, Milan, Italy), and filtered water. Glycemia and glycosylated haemoglobin A1 (HbA1c) were measured through tail-vein blood sampling and detection with Bayer A1C Now+ (Cat. No. 08842610) and a blood glucose meter (71371-80, FreeStyle Optium Neo; Abbott).

All animal experiments were conducted in agreement with the European Community (86/609/CEE) and the guidelines of the Association for Research in Vision and Ophthalmology (ARVO) for the utilization of laboratory

animals. The Animal Care and Use Committee of VHIR (CEEA 14/21) authorized the present study.

### Expansion

The expansion of endogenous Treg was performed as previously described [20] through the injection of IL-2/anti–IL-2 mAb (JES6-1) complexes. Briefly, recombinant mouse IL-2 (PeproTech, 1 µg per animal; Cat. No. 212−12) was mixed with either anti–IL-2 monoclonal antibody (mAb) (clone JES6-1; BE0043; Abyntek; 5ug per animal, referred as Treg group) or its isotype control (rat IgG2a, referred to as "isotype" group from here on), and incubated at 37 °C for 30 min. 9-week-old mice were injected intraperitoneally (i.p.) in a final volume of 200uL. Mice received a daily injection for 3 consecutive days on the first week and then a reminder injection once a week for 5-weeks (Summarised in Figure S1A). An additional group of db/db animals non-injected was added to the study to ascertain possible alterations driven by the isotype treatment in comparison to basal db/db mice. Animals were 18 weeks at the end point of the experiment, representing an established but not yet advanced stage of diabetes.

Nine-weeks after the first expansion, mice were terminally anaesthetised with i.p. Ketamine (75 mg/kg) and Xylacine (12 mg/kg) injection and transcardially perfused with ice-cold phosphate buffered saline (PBS) followed by 4% paraformaldehyde (PFA) (Sigma-Aldrich). Eyes were enucleated and immersed in 2% PFA for 2 h. Then, eyes reserved for cryosectioning were cryoprotected with 30% sucrose in PBS for 72 h, snap-frozen in OCT (Tissue-Tek, Sakura Finetek, Cat. No. 4583), cryosectioned at 15 µm thickness and immunostained as indicated below. Eyes that were used for flatmount staining were fixed overnight and transferred to PBS. Eyes for western blot were dissected and immediately frozen.

### In vivo fundus imaging

All procedures were conducted under general anesthesia with a mixture of 2% isoflurane (Arrane®. Baxter laboratories, Victoria, Australia)/1% O2 using an induction camera and a rodent mask. Body temperature was maintained with a heating pad. Pupils were dilated with Tropicamide eyedrops (Colorcusi Tropicamida® 10 mg/mL, Alcon Laboratories, El Masnou, Spain), and 2% Methocel gel (OmniVision, Puchheim, Germany) was administered to the cornea to favor contact with the lens. Animals were subjected to fundus fluorescence angiography (FA) on the week prior to the end point. Once the animals were anesthetized and pupils dilated, 10 µL/g sodium fluorescein (0.1% Fluorescein Oculos, Thea Laboratories, S.A., Spain) was administered intraperitoneally. Eye fundus images from the central retina were taken 1 min after fluorescein administration using the Micron III platform (Phoenix Research Labs., Pleasanton, CA, USA).

### Flow cytometry

#### *Blood, spleen and retina*

Treg levels were investigated in the blood, spleen and retina of all groups by flow cytometry at the time points specified in Figure S1A. In brief, spleens were mashed through a 70 µm strainer and then treated with red blood cell lysis buffer (STEMCELL Technologies) for 2 min at room temperature. Cells obtained from spleens were then washed with PBS and centrifuged at 300 g for 5 min at 4 °C. Cells were resuspended in 200 µL PBS and stained with a cell viability dye with eFluor 506 viability dye (1:500; Thermo Fisher Scientific, Cat. No. 65-0866-18) and cell surface stained with antibodies for CD45 (eBioscience, clone 104, Cat. No. 47-0454-82), CD4 (1:500; eBioscience, clone GK1.5, Cat. No. 17-0041-81), CD25 (1:500; eBioscience, clone PC61.5, Cat. No. 12-0251-82), CD3 (1:500; eBioscience, clone 17A2, Cat. No. 11-0032-82), all 1:500, for 15 min at RT. Cells were washed with flow cytometry wash buffer (PBS) and centrifuged at 300 g for 5 min at 4 °C. Cells were then fixed with Fix & Perm A (Thermo Fisher Scientific, Cat. No. GAS004) for 10 min at RT. Fixative was washed off with PBS and centrifuged at 300 g for 5 min at 4 °C. Then, cells were resuspended in 100 µL Fix & Perm B (Thermo Fisher Scientific; Cat. No. GAS004) with an anti-Foxp3 antibody (1:100; eBioscience, clone FJK-16 S, Cat. No. 48-5773-82) and T-bet antibodies (1:100, eBioscience, clone eBio4B10 (4B10), Cat. No. 45-5825-82) overnight at 4 °C. Cells were then washed with PBS and centrifuged at 300 g and 4 °C for 5 min. Final pellet was resuspended, data were acquired on a Fortessa (LSRFortessa™ High-Parameter Flow Cytometer, BD Biosciences) and analysed using FlowJo software version 10.0 (BD). To calculate Treg percentages, singlets were identified by FSC-H versus FSC-A and viable cells gated on $CD4^+CD3^+$ expression, and within the $CD4^+$ population Treg markers $Foxp3^+$ was delineated.

#### *Blood*

Blood obtained from the animals at the time of perfusion was collected in EDTA-tubes to avoid blood coagulation. 30 µl of the blood were incubated with surface antibodies in PBS as indicated per spleen for 15 min at RT. Cells were washed with flow PBS and centrifuged at 300 g for 5 min at 4 °C. Red blood cells were then lysed and cells were fixed with Optilyse B (Beckmann and Coulter; Product No: IM1400) for 10 min at RT. Fixative was washed with ddH20 to finish red blood lysis for 15 min and centrifuged at 300 g for 5 min at 4 °C. Then, cells were resuspended in Fix & Perm B (Thermo Fisher Scientific) with an anti-Foxp3 antibody (1:100; eBioscience,

clone FJK-16 S) and T-bet antibodies (1:100, eBioscience, clone eBio4B10 (4B10)) overnight at 4 °C. Cells were then washed with FCSB and centrifuged at 300 g and 4 °C for 5 min. The final pellet was resuspended, data were acquired on a Fortessa and analysed using FlowJo software version 10.0 (BD). Treg percentages were calculated as indicated above.

#### *Retina*

Retinas were dissected from enucleated eyes and separated from the RPE choroid. Retinas of two eyes from the same animal were put together, cut into small pieces and subjected to papain (Worthington) digestion for 30 min at 37 °C in hibernate A with DNAse type I (Worthington). Upon digestion papain was washed-off with Hanks Buffered Salt Solution (HBSS) (Thermo Fisher Scientific) and cells were centrifuged at 300 g for 5 min at 4 °C. The pellet was resuspended in 4 ml trituration buffer (Hibernate A with 2% B27 (Gibco Life Technologies; Cat. No. 17504044) and 4mM Sodium Pyruvate (Thermo Fisher Scientific) and gently triturated with a 5mL serological pipette. Cell suspension was transferred to a 50mL tube through a 70 µm strainer and the remaining tissue resuspended in another 2 ml of trituration buffer and gently triturated using a fire-polished glass pipette. After trituration supernatant was again transferred to a 50mL tube through a 70 µm strainer. This step was repeated again twice, with a glass pipette of decreased diameter and a 1mL pipette tip. Cells were resuspended in 250 µl PBS and stained following the same protocol as the spleen. Data was acquired on a Fortessa and analysed using FlowJo software version 10.0. Considering the limited number of Treg in the retina, to adequately find the population, CD45 and CD4 gates were established and then $CD4^+$ cells from each mouse were grouped (concatenated) based on the received treatment (db/+, db/db with Isotype and db/db with Treg). Within each treatment group the same number of $CD4^+$ cells were selected (508 cells per group) using downsample plugin in FlowJo. This allowed to group a higher number of $CD4^+$ T cells, facilitating the identification of the $Foxp3^+$ Treg population within the retina despite its low number. Treg population was identified by positively selecting $Foxp3^+$ cells within $CD4^+$ population. Both, the percentage of $Foxp3^+$ cells as well as the number of Foxp3+events within $CD4^+$ T cells were established per treatment group. The number of total Foxp3+events were graphed in an histogram representing the counts for $Foxp3^+$ events against the Foxp3-e450 intensity per group. Once the gate was established Treg count per group within the $CD4^+$ gate was obtained and the percentage of $Foxp3^+CD4^+$ Treg was established per individual animal.

### Immunostaining

#### *Cryosection staining*

Cryosection staining was performed as previously described [21]. Briefly, eye sections were dried for 30 min at RT and washed in PBS for 10 min. Antigen retrieval was performed using Citrate buffer pH 6.0 (Abcam, ab93678) at 95ºC for 5 min in a water bath and after cooling, and additional 5 min with 10% SDS. Slides were then blocked in 10% Donkey serum (Sigma Aldrich, D9663) with 0.2% Triton-X in PBS for 1 h at room temperature. Primary antibodies (Table 1) were added and incubated overnight at 4ºC in 0.5% donkey serum and 0.2% Triton-X followed by incubation with secondary antibodies (Table 1) for 1 h at room temperature, in PBS.

#### *Flatmount staining*

The retinal flatmount tissues were first washed in PBS, followed by permeabilization with 2% Triton-X 100 overnight at 4 °C. Afterward, the samples were blocked using 5% donkey serum in 0.2% Triton-X 100 with 1mM $CaCl_2$, incubating overnight at 4 °C. They were then treated with the appropriate primary antibody (Table 1) diluted in 0.2% Triton-X PBS for 96 h at 4 °C. Following a 6-hour wash, the tissues were incubated overnight at 4 °C with the relevant secondary antibodies (Table 1), washed again for 6 h, and finally mounted for analysis.

### Image acquisition and analysis

Tissue sections were cover-slipped with Vectashield (Vector Labs, Cat. No. H-1000-10) and examined by Leica Thunder DMi8 or confocal microscope (Zeiss LSM980, Jena, Germany). Consistent cryosectioning patterns were applied across all animals using the same slides for each histological marker analysed and ensuring that all retinal sections were obtained from the middle-center eccentricities to minimize variability and potential positional errors. Images were captured from 3 to 4 regions across 2–4 different sections of the middle-center retina. Further image processing and analysis was performed using Fiji software and blindly manually counted.

### Western blot

Samples were homogenized sonicating the frozen retinas in 70µL of RIPA buffer containing protease inhibitor cocktail (Sigma, Cat. No. 04693159001 and R0278, respectively) and PhosSTOP™ (Roche, Cat. No. 04906837001). Protein concentration was determined using a Bradford Assay (Thermo Fisher Scientific, Cat. No. 23246). The blot was performed using 60 µg of protein according to previously described methods [12] but with nitrocellulose membranes. Primary and secondary antibodies used are detailed in Table 1. Membranes were visualized with enhanced chemiluminescence WesternBright ECL HRP substrate kit

**Table 1** Antibodies used in the study

| **Primary antibody** | **Cat. No.** | **Company** | **Host** | **Dilution** |
|---|---|---|---|---|
| Brn3a Antibody (C-20) | sc-31,984 | Santa Cruz Biotechnology | Goat | 1:200 |
| Ionized calcium binding adaptor molecule 1 (IBA-1) antibody | ab5076 | Abcam | Goat | 1:200 |
| Recombinant Anti-PKC alpha antibody [133] | ab11723 | Abcam | Mouse | 1:500 |
| Anti-Cone Arrestin Antibody | AB15282 | Sigma | Rabbit | 1:500 |
| Guinea Pig Anti-Synaptophysin | AGP-144 | Alomone | Guinea Pig | 1:150 |
| Anti-Glial Fibrillary Acidic Protein antibody (GFAP) | Z0334 | Agilent | Rabbit | 1:500 |
| Biotinylated Isolectin B4 | VEC.B-1205 | Vector Labs | Biotin | 1:50 |
| Albumin | a90-134a | Bethyl | Goat | 1:100 |
| DAPI (4′,6-diamidino-2-phenylindole) | D3571 | ThermoFisher | | 1:1000 |
| Tyrosine hydroxylase (TH) antibody | AB152 | Merck | Rabbit | 1:100 |
| Choline acetyltransferase (ChAT) | Ab144P | Merck | Goat | 1:100 |
| Recombinant Anti-NLRP3 antibody | ab270449 | Abcam | Rabbit | 1:500 |
| Vinculin antibody | sc-73,614 | Santa Cruz Biotechnology | Mouse | 1:1000 |
| GAPDH antibody | ab8245 | Abcam | Mouse | 1:1000 |
| IL-18 (H-173) antibody | sc-72,954 | Santa Cruz Biotechnology | Rabbit | 1:500 |
| Caspase-1 Antibody and p20 | #2225 | Cell Signaling | Rabbit | 1:1000 |
| RBPMS | PA5-115831 | ThermoFisher | Rabbit | 1:100 |
| CD68 | ab53444 | Abcam | Rat | 1:100 |
| Tmem119 | ab209064 | Abcam | Rabbit | 1:100 |
| **Secondary antibody** | **Company** | **Cat. No.** | | |
| Donkey anti-Rabbit IgG (H + L) Highly Cross-Adsorbed Secondary Antibody, Alexa Fluor 568 | ThermoFisher | A10042 | | |
| Donkey anti-Rabbit IgG (H + L) Highly Cross-Adsorbed Secondary Antibody, Alexa Fluor 647 | ThermoFisher | A-31,573 | | |
| Donkey anti-Mouse IgG (H + L) Highly Cross-Adsorbed Secondary Antibody, Alexa Fluor 488 | ThermoFisher | A21202 | | |
| Donkey anti-Mouse IgG (H + L) Highly Cross-Adsorbed Secondary Antibody, Alexa Fluor™ 647 | ThermoFisher | A32787 | | |
| Donkey anti-Goat IgG (H + L) Cross-Adsorbed Secondary Antibody, Alexa Fluor™ 568 | ThermoFisher | A11057 | | |
| Donkey Anti-Goat IgG H&L (Alexa Fluor® 488) (ab150129) | Abcam | ab150129 | | |
| Donkey Anti-Goat IgG H&L (Alexa Fluor® 647) (ab150131) | Abcam | ab150131 | | |
| Goat anti-Guinea Pig Alexa Fluor 568 | Abcam | ab175714 | | |
| Goat Anti-Rabbit Immunoglobulins/HRP | Agilent DAKO | P0448 | | |
| Streptavidin, Alexa Fluor™ 647 conjugated | ThermoFisher | s21374 | | |

(Advansta, K-12045-D50CA) and bands detected using LI-COR Licor Odyssey FC 2800 Western Blot Imaging System (LICORbio).

### Immunoassays

#### *HbA1 and insulin quantification*

Plasma insulin levels were determined using an ultrasensitive mouse enzyme-linked immunosorbent assay (10-1251-01, Mercodia Inc., Winston-Salem, NC, USA).

#### *Magnetic bead-based immunoassay for retinal VEGF detection*

Protein from retinas were extracted by sonicating the isolated tissue in RIPA buffer containing protease inhibitor cocktail (Sigma) and PhosSTOP™ (Roche). Protein concentrations were determined by using Pierce BCA protein assay kit (Thermo Fisher Scientific, Cat. No. 23225).

VEGF concentration in 100 µg of retinal homogenates was determined using the ProcartaPlex Mouse and Rat Mix & Match kit (Thermo Fisher Scientific, PPX-10-MXT2CFM) following the manufacturer's instructions. Samples were processed in a 96-well flat bottom plate and analysed with a Luminex MAGPIX instrument (Luminex Corporation, Austin, TX, USA) utilizing xPONENT 4.2 software (Luminex Corporation). The MAGPIX system employs a sandwich ELISA methodology, where the capture antibody is attached to fluorescently dyed magnetic microspheres, facilitating bead-based quantitative protein detection. The protein concentration was derived from standard curves through five-parameter logistic (5 PL) curve fitting conducted by the software.

### Statistical analysis

Statistical analysis was performed using Graph Pad Prism (GraphPad Software, Inc. version 10). First, normal

distribution was assessed using Kolmogorov-Smirnov tests. When the data was described as percentage, an *arcsin* conversion was performed to analyse the data using parametric tests for normally distributed data. When only two groups were compared, e.g. Treg percentage changes upon Treg expansion, Student t-test was used. For comparisons involving more than two groups, 1-way ANOVA analysis was performed followed by Tukey's multiple comparisons test. For all statistical tests, differences were considered significant with p values below 0.05.

## Results

### db/db mice have a systemic and retinal decrease in Treg proportions which are recovered after systemic expansion

Due to the lack of consensus regarding the alteration in Treg cell numbers in T2D patients [22–24], our initial objective was to ascertain whether Tregs are altered in db/db T2D mice. In blood, db/db animals present almost half the percentage of $Foxp3^+CD4^+$ cells within their $CD4^+$T lymphocytes than their control counterparts, the db/+ animals (Figure S1B). To overcome this decrease, we systemically expanded endogenous Treg following the protocol described by Webster et al. [20] with minor modifications (Figure S1A). We confirmed Treg expansion upon IL-2/mAb IL-2 treatment in blood 4–5 weeks after the initial injection (half-way the treatment) (Figure. S1C) and 9-weeks after the experiment (experimental endpoint) (Figure S1D).

Considering that Treg numbers in the healthy retina are very low [21], we next determined whether the impact of Treg expansion was detectable in the retina. As described for peripheral Treg, db/db mice showed a decrease proportion of Treg and Treg number within the $CD4^+$ T cell population in the retina. Similarly to blood and spleen, despite still being found in small numbers, as described before [21], IL-2 mediated Treg systemic expansion was also effective in the retina [25] (Figure S1E-G).

Once local and systemic Treg expansion were confirmed, we next sought to determine if systemic Treg expansion in db/db mice had any consequence in metabolic control including hyperglycemia, HbA1c and blood insulin levels. Treg expansion did not significantly change these parameters, (Figure S2A-C, respectively).

### Treg expansion prevents retinal neurodegeneration in db/db mice

We next aimed to determine whether Treg expansion rescued changes in retinal pathology and neurodegeneration that are characteristic of db/db mice. Histological analysis using hematoxylin-eosin staining revealed a significant decrease in total retinal thickness in both non-injected db/db mice and db/db animals receiving isotype treatment, in line with previous reports [26]. This reduction of retinal thickness was not observed in the Treg-expanded group. The retinal thinning in db/db and isotype-treated mice primarily resulted from decreased thickness in the innermost layers, particularly the inner plexiform layer (IPL) and inner nuclear layer (INL). In contrast, the db/db mice undergoing Treg expansion exhibited no significant loss of IPL or INL thickness, and their retinal layers appeared similar to those of non-diabetic db/+ mice (Fig. 1A-B).

It is well-established that the altered vision associated with DR in db/db is linked to neurodegenerative pathology, including loss of photoreceptors, amacrine cells and retinal ganglion cells (RGC) [26, 27]. Thus, to determine the effect of Treg expansion in these defined retinal neuronal populations, we examined the changes in the total number of photoreceptors ($DAPI^+$ cell rows) in the ONL and Cone Arrestin (CA) (Fig. 1C-E). We observed a significant decrease in the total number of photoreceptors in both diabetic non-injected and isotype injected animals, which was not present in animals that underwent Treg expansion. When looking at cone photoreceptors, we observed a slight but significative reduction in number in isotype-injected db/db, not present in Treg expanded. These results suggest that the reduction of photoreceptors seen in diabetic animals, whether they were non-injected (db/db) or isotype-injected, appears to be primarily linked to a reduction in rod photoreceptors. This loss was not observed in animals with Treg expansion.

To further explore the effect of Treg expansion on diabetic neurodegeneration, we also examined rod bipolar second-order neurons (Fig. 1F-H). In healthy retinas (db/+), rod bipolar cell bodies are positioned in the outer region of the INL, near the OPL. In non-injected diabetic mice (db/db), there was a mild but significant reduction in the total number of $PKC\alpha^+$ somas across the INL (Figure S4A). Degenerative changes, such as shorter and distorted processes and fewer cell bodies [21, 28, 29], were evident in both non-injected and isotype-treated diabetic retinas. Specifically, near the OPL, both groups had fewer $PKC\alpha^+$ somas, while the number of $PKC\alpha^+$ somas in Treg-expanded diabetic mice was comparable to that in non-diabetic db/+ mice (Fig. 1F, G). Beyond changes in cell number near the OPL, $PKC\alpha^+$ rod-bipolar cells showed altered laminarity, with a significant increase in ectopic $PKC\alpha^+$ somas located below the OPL, due to shorter axons, in both non-injected and isotype-treated db/db mice that was absent in non-diabetic db/+ and Treg expanded diabetic animals (Fig. 1F, H). We also observed bipolar dendrites and synaptophysin sprouts areas extending from the OPL towards the ONL, a recognised sign of neurodegeneration [28], in both non-injected control and isotype db/db mice, which were absent in diabetic animals that underwent Treg

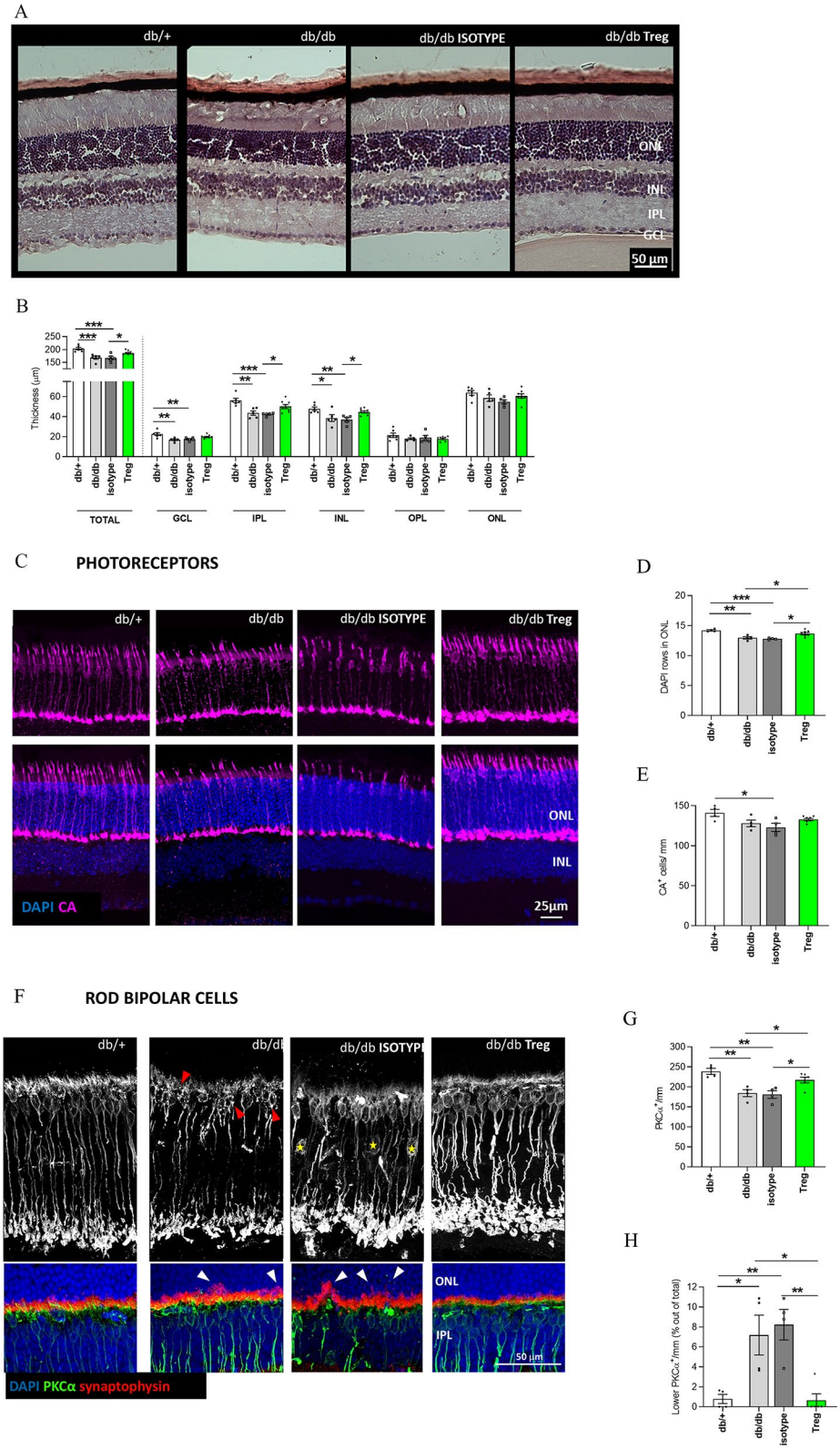


**Fig. 1** (See legend on next page.)

(See figure on previous page.)

**Fig. 1** Treg expansion limits DR neurodegeneration. **A-B**, Hematoxylin and eosin analysis of retinal thickness. Representative images showing hematoxylin and eosin staining of db/+, db/db non-injected and db/db injected with either IL-2/mAb IL or its control (**A**). Quantification of the total retinal layer thickness as well as the thickness of the different cell layers (**B**). Scale bar is 50 µm. $n = 5–8$ mice. **C-E**, Immunostaining and quantitative analysis of photoreceptors. Representative images showing photoreceptors in the ONL (**C**) (Cones, $CA^+$) in diabetic db/db animals non-injected, injected with the isotype, db/db animals receiving a Treg expansion and non-diabetic db/+ (scale bar = 25 µm). Quantitative analysis of the number of rows of $DAPI^+$ nuclei in the ONL (**D**). Quantification of the number of cone photoreceptor cells (**E**) ($CA^+$ cells) $n = 4–5$ animals. **F-H**, Immunostaining and analysis of rod bipolar cells and synaptic vesicles. Representative image of PKC-α (**F**) (upper panel, grey. Lower panel, green) and synaptophysin (red, lower panels). Stars indicate abnormal location of some PKC-$\alpha^+$ cell soma lower within the INL. Arrowheads indicate abnormal rod bipolar dendrite and synaptic vesicles sprouts into the ONL (scale bar = 25 µm). Quantitative analysis of the number of PKC-$\alpha^+$ somas close to OPL (**G**) ($n = 4–6$ mice) and (**H**), percentage of PKC- $\alpha^+$ somas found in a lower location out of the total of PKC-$\alpha^+$ cells ($n = 4–6$ animals). Data expressed as mean ± s.e.m. 1-way ANOVA followed by Tukey's multiple comparisons test. * $P < 0{,}05$; ** $P < 0{,}01$; *** $P < 0{,}005$; **** $P < 0{,}001$

expansion and in non-diabetic db/+ mice (Fig. 1F, white arrowheads).

To further address potential cellular changes linked to neurodegeneration in DR, we next examined retinal interneurons. Although no changes were observed in calbindin$^+$ horizontal cells (Figure S4B), alterations were evident in amacrine cells of db/db animals (Fig. 2A-C). We observed a decrease in the number of $ChAT^+$ (Fig. 2A, upper panel, and 2B) and $TH^+$ (Fig. 2A, lower panel, and 2 C) somas, representing cholinergic and dopaminergic amacrine cells, respectively. This finding aligns with previous reports from various experimental models of diabetic retinopathy [29–31]. Diabetic animals that underwent Treg expansion showed a significantly higher number of $ChAT^+$ and $TH^+$ amacrine cells, in line with the numbers observed in db/+ mice (Fig. 2A-C). Likewise, the decrease in displaced cholinergic amacrine cells observed in both db/db and isotype treated diabetic groups was absent in diabetic animals that underwent Treg expansion (Fig. 2A, D).

Lastly, we examined alterations in the retinal ganglion cell layer (GCL) due to the endogenous expansion of Treg in T2D animals (Fig. 2E-H). Treg-expanded diabetic animals exhibited a significant increase in the total number of $DAPI^+$ cells in the GCL compared to their non-expanded diabetic controls. Notably, the total number of $DAPI^+$ cells in the GCL of Treg-expanded diabetic animals was comparable to that of db/+ non-diabetic animals (Fig. 2E, F). As previously described, non-injected db/db mice presented fewer RGC cells ($RBPMS^+$ cells) and $Brn3a^+$ RGC when compared to non-diabetic db/+ mice (Fig. 2G and **H**, respectively). This decrease was also observed in the isotype treated db/db mice, while the expansion of Treg showed a significant increase in the number of total RGC cells ($RBPMS^+$ cells) and $Brn3a^+$ RGCs, bringing numbers up to those of non-diabetic db/+ mice (Fig. 2E, G and **H**).

#### Treg expansion reduce gliosis and retinal inflammation

We next studied the consequences of Treg expansion in the microglia and Müller cells that are responsible for initiating and perpetuating inflammation in DR [32, 33]. As expected, we observed an increased number of Iba-$1^+$ cells, the majority of which were $Tmem119^+$ (Figure S4C, D), indicating that they were microglial cells, in both non-injected control and isotype-treated diabetic animals compared to non-diabetic controls. Treg expansion significantly decreased Iba-$1^+$ microglial cells in the db/db retina, to levels that were comparable to non-diabetic controls (Fig. 3A-B). This finding is consistent with observations from retinal flatmounts (Fig. 3C). In line with our previous findings, the number of Iba-$1^+$ microglial cells in the INL was elevated in isotype-treated diabetic animals, but this increase was significantly reduced following Treg expansion, bringing the levels closer to those observed in non-diabetic controls (Figure S4E).

Increased expression of glial fibrillary acidic protein (GFAP) as a response of reactive gliosis, is one of the earliest and more prominent signs of Müller cells activation in DR. db/db mice subjected to Treg expansion showed a significant reduction in the number of $GFAP^+$ filaments that crossed the IPL when compared to either isotype or non-injected db/db animals (Fig. 3C-D).

Inflammasomes are central regulators of innate immunity, and their involvement in several neuroinflammatory pathologies has been widely described [34]. In the diabetic eye, the NLRP3 inflammasome has been shown to be activated within the retina, specifically in Müller cells, which are a primary source of NLRP3 [35, 36]. Thus, considering the decreased gliosis observed in DR upon Treg expansion, we next examined the expression of NLRP3 inflammasome in the retina (Fig. 3E, F). NLRP3 protein levels were significantly increased in isotype-treated diabetic animals, while animals exposed to Treg expansion present similar NLRP3 protein levels to those of non-diabetic db/+ mice. This was further confirmed by assessing the protein levels of two key downstream effectors of the NLRP3 inflammasome pathway: IL-18 and Caspase-1, including the cleaved form, Caspase-1 p20. All three—IL-18, Caspase-1, and Caspase-1 p20—were significantly reduced in db/db animals subjected to Treg expansion compared to isotype-treated db/db animals (Fig. 3G and H, J, respectively).

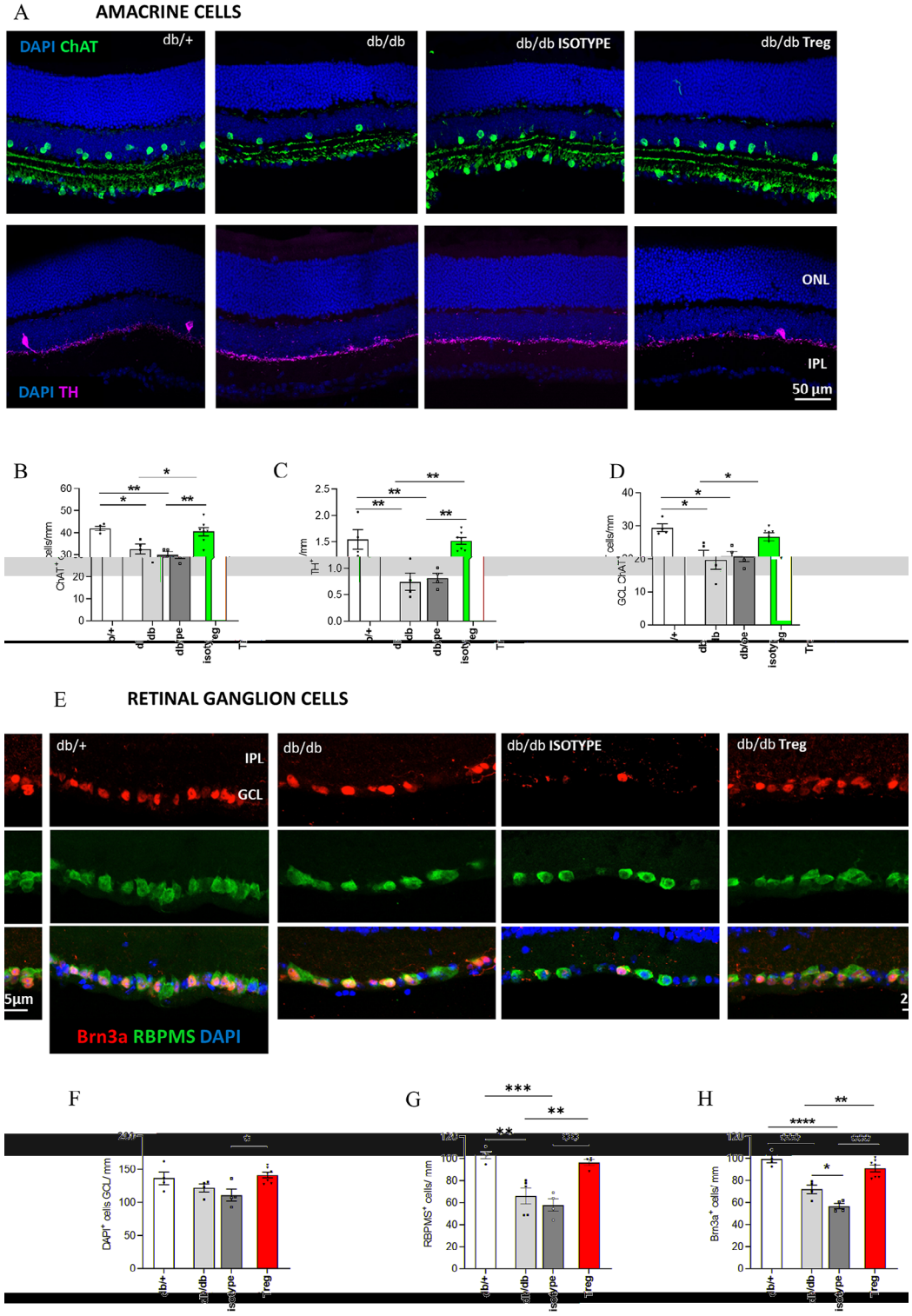


**Fig. 2** Effect of Treg cell expansion on DR-related neuronal damage. **A-C**, Immunostaining and quantitative analysis of cholinergic (ChAT$^+$) and dopaminergic (TH$^+$ cells) amacrine cells. **A**, Representative image of Chat$^+$ cells (green, upper panel) and TH$^+$ amacrine cells (purple, lower panel) (Scale bar = 50 µm). **B**, **C**, quantification of the number of ChAT$^+$ (**B**) and TH$^+$ (**C**) somas per mm of retina. **D**, quantification of the number of displaced ChAT$^+$ amacrine cells into the GCL. $n = 4–7$. **E-H**, Immunostaining and analysis of retinal ganglion cells (RGC). **E**, Representative image of RBPM and Brn3a$^+$ RGC (Scale bar = 25 µm). **F**, Quantification of the number of DAPI$^+$ cells in the GCL; **G-H**, quantification of RBPMS and Brn3a$^+$ RGC, respectively. Data presented as mean ± s.e.m. *$P < 0.05$; ** $P < 0.01$; ***$P < 0.001$; 1-way ANOVA followed by Tukey's multiple comparisons test

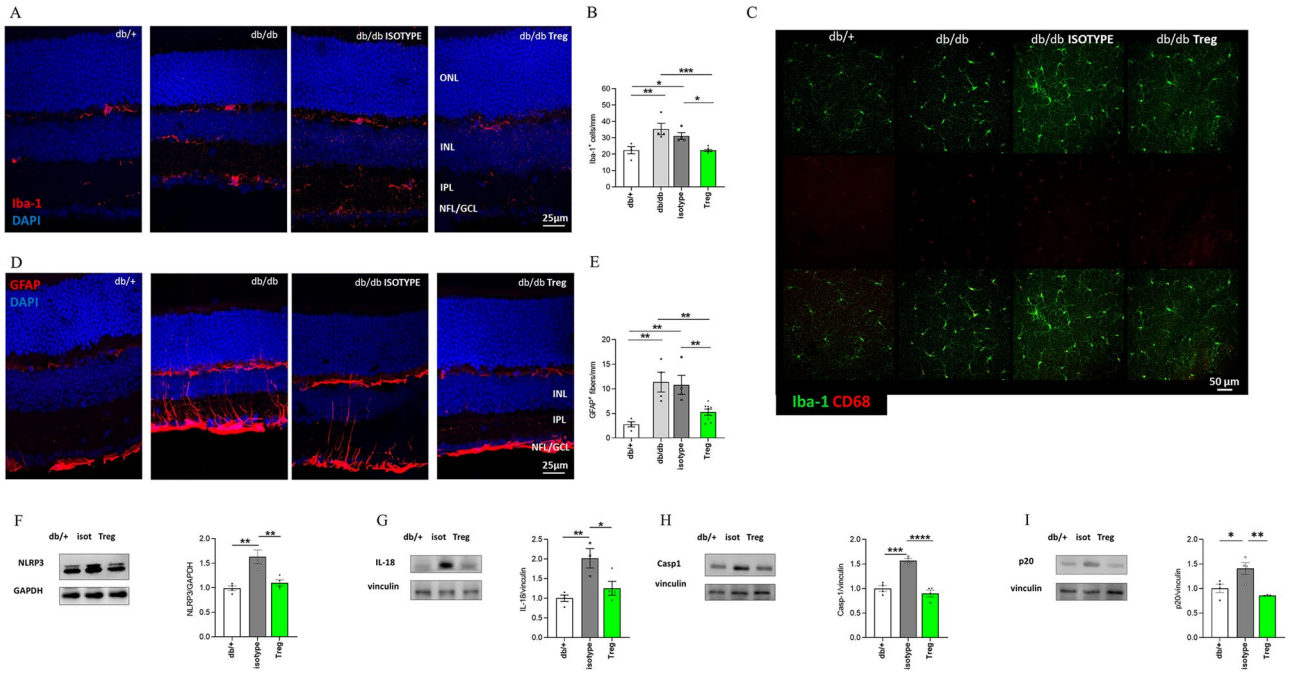


**Fig. 3** Animals undergoing Treg expansion exhibited reduced DR-related inflammatory features. **A-E** Analysis of Iba-1$^+$ microglial cells and GFAP$^+$ Müller cells determined by immunofluorescence. Representative image of microglial cells in sections (**A**) (Iba-1$^+$, red), in retinal flatmounts (**C**) (Iba-1 green, CD68 red) and **D**, gliotic Müller cells (GFAP$^+$ fibers, red). Scale bars = 25 µm in sections; 50 µm in flatmount). **B**, Quantitative analysis of the total number of Iba-1$^+$ cells in all layers of the retina. **E**, number of GFAP$^+$ fibers crossing the IPL per mm. $n = 4–8$. **F-I**, Western blot analysis and representative blot of NLRP3 (**F**), mature form of IL-18 (**G**), Caspase-1 (**H**) and p20 Caspase-1 cleaved form (**I**) ($n = 4$). Data presented as mean ± s.e.m. *$P < 0.05$; ** $P < 0.01$; ***$P < 0.005$; 1-way ANOVA followed by Tukey's multiple comparisons test

### Peripheral Treg expansion improves diabetic retinopathy vasculopathy

Vascular damage is a hallmark of DR. To investigate this, we performed in-vivo fundus angiography with sodium fluorescein, which revealed markedly tortuous retinal vessels in db/db mice, both in non-injected and isotype-treated groups (arrows, Fig. 4A). This feature is reflective of the vasodegenerative pathology in DR [37] but was absent from db/db mice that underwent Treg expansion (Fig. 4A).

To determine if the inner blood retinal barrier was affected, as previously described in db/db mice [12, 38], we performed immunostaining with isolectin B4 and albumin with subsequent quantification of the number and size of the leakage spots, reflecting areas where blood-borne albumin had leaked into the neuropile (Fig. 4B-E). As shown in Fig. 4B-C, db/db non-injected animals or mice receiving the isotype exhibited several large, focal leakage areas (indicated with white arrowheads, Fig. 4B and Figure S4F-G in retinal flatmounts), while db/db mice with expanded Treg showed less and smaller leakage spots (Fig. 4B, yellow arrowhead; Fig. 4D and E, respectively and Figure S4F-G in retinal flatmounts). These findings indicate that Treg expansion ameliorates the diabetes-induced blood-retinal barrier breakdown. Since VEGF, also named vascular permeability factor, plays an essential role in inducing vascular leakage in diabetic retina [39], we also investigated changes in this pivotal factor in our study. We found that control db/db mice showed an expected increase in the concentration of this growth factor that was absent in animals subjected to Treg expansion, with levels closer to those of db/+ mice (Fig. 4E).

## Discussion

In this study we found a marked reduction of Tregs in db/db mice, a model of T2D that features hyperglycemia, insulin resistance [40], and early stages of DR [26]. Systemic Treg expansion led to increased retinal Tregs and prevented key DR hallmarks, such as neuron loss, glial activation, and vascular leakage. These effects could not be attributed to an improvement of blood glucose levels. This highlights Tregs as a potential new immunomodulatory approach to prevent retinal damage in DR.

Low-grade inflammation is a well-known underlying pathogenic factor of T2D, leading to several studies investigating Treg cells in the context of T2D. A systematic review and meta-analysis indicated that patients with T2D have a lower percentage of peripheral CD4$^+$Foxp3$^+$ Tregs compared to healthy controls, with even lower levels in those with complications [22]. However, other studies have reported not a decrease

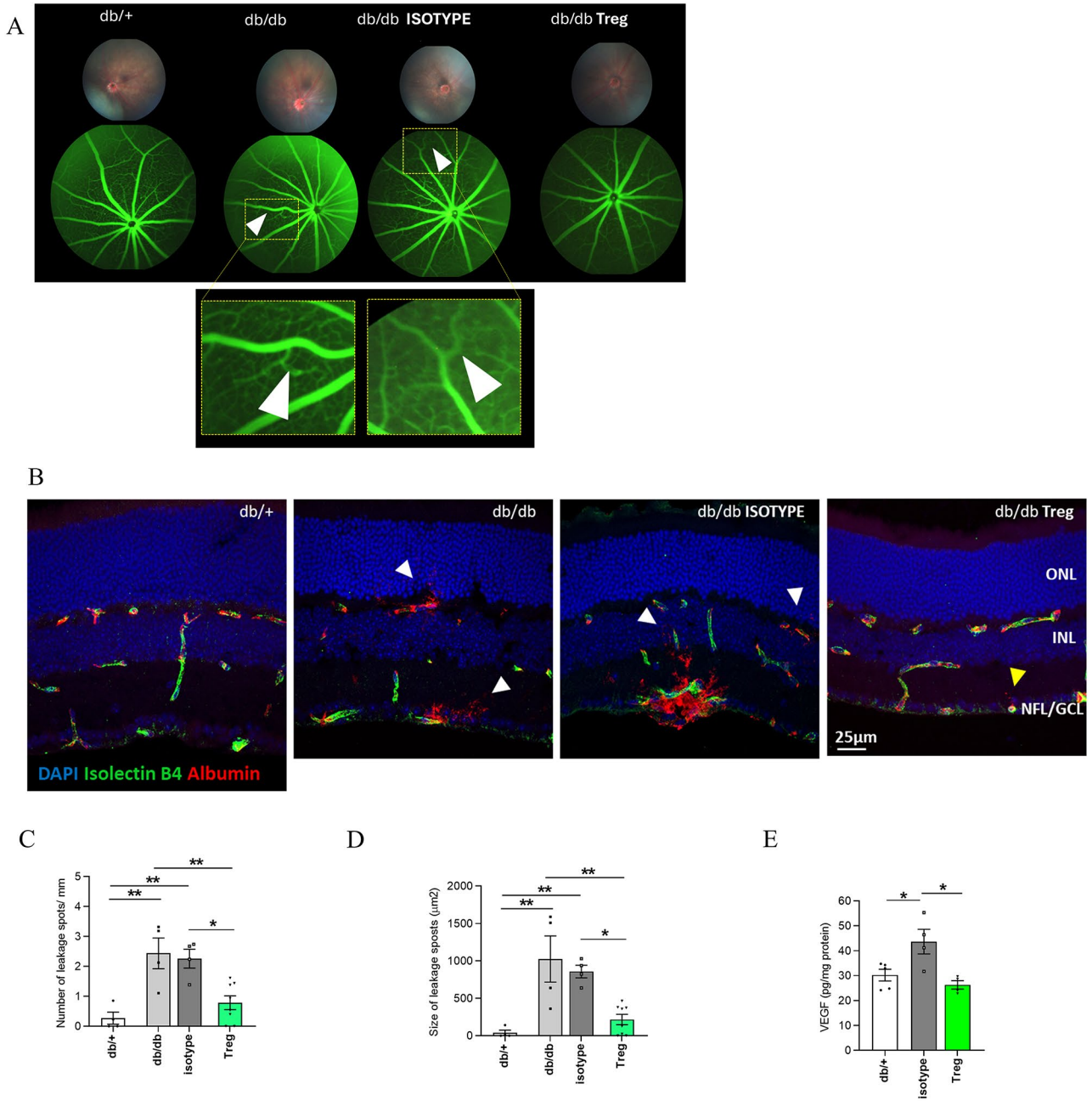


**Fig. 4** Treg expansion reduces diabetes-associated vascular damage and alteration of thickness. **A**, Fundus fluorescein (fluorescein sodium) image of db/+, db/db and db/db receiving either IL-2/anti-IL-2 or its isotype. In yellow, magnified image of the area. The arrowhead indicates vascular tortuosity in db/db animals and and db/db treated with IL-2/isotype. **B-D**, Representative images of retinal sections (**B**) showing retinal barrier leakage, visualized using isolectin B4 (green) and albumin (red) staining. The quantification includes the number of leakage spots per mm of retina (**C**) and the average size of the leakage spots (in $\mu m^2$) (**D**). The leakage spots/areas were determined by counting the number of albumin$^+$ and isolectin B4$^-$ spots and measuring the area of albumin$^+$ regions in retinal sections. White arrowheads indicate larger or more extensive areas of leakage, while yellow arrowheads mark smaller areas of leakage. Scale bar 25 µm. $n = 4–8$ (**C**) and $n = 3–6$ (**D**). **E**, Quantification of VEGF concentration in the retina, normalized to the total protein in the retina. $n = 4–5$. Data presented as mean ± s.e.m. $^*P < 0.05$; $^{**}P < 0.01$; 1-way ANOVA followed by Tukey's multiple comparisons test

in the percentage of Tregs but rather an imbalance between Th17 and Treg cells [24], or a reduction in Treg functionality [41]. Despite the conflicting data, it seems plausible that alterations in Treg cells, either in reduced numbers or decreased functionality, could contribute to the inflammatory environment characteristic of T2D. In experimental models of T2D, including studies with db/db mice, Treg levels have been sparsely studied, with results showing some variability that may depend on the specific mouse strain and T2D model

utilized [42, 43]. In the present study we have observed less $CD4^+CD25^+Foxp3^+$ Treg in the blood of db/db mice compared with non-diabetic animals. This is particularly relevant considering the resemblance of this model with human T2D features. In an experimental model of T2D, Treg had been shown to reverse or improve insulin resistance [44]. However, we did not observe any significant changes in hyperglycemia, HbA1c, or circulating insulin. These findings strongly suggest that the observed effects in the retina are independent of any changes in the diabetic status of the animals. Instead, they can be attributed to the immunosuppressive and potentially to their suggested role in supporting neuronal health, as indicated in the literature and possibly relevant to the effects observed in this study [13–15]. Nonetheless, we cannot rule out that a different treatment regimen or a different Treg approach could influence the metabolic control or even the course of T2D and its associated complications.

Several investigations have demonstrated that Treg are integral to immune regulation, tissue regeneration and neuroprotection within the CNS, however, very few studies have specifically focused on their role in the retina [13, 21, 25]. While CNS has traditionally been considered as immune privileged, recent findings indicate the presence of Treg within the healthy CNS, including the retina, albeit in minimal quantities [21]. This suggests that Treg may possess mechanisms enabling them to traverse the blood-brain and blood-retinal barriers. In fact, Treg are actively recruited to the retina to repair pathological angiogenesis [25]. In addition, we have recently described a role of Treg in preserving retinal homeostasis and thereby restraining age-related degenerative changes [21], which share some common hallmarks with DR, such as neurodegeneration, inflammation and gliosis. On this basis it is tempting to speculate that the reduced systemic Treg reported in diabetes, and particularly its deficit in the retina, could be involved in the development and progression of DR. Our finding showing that Treg expansion was not only detected in blood and spleen but also in the retina of db/db mice, indicates that Treg have the capacity not only to migrate to the retina but to exert a myriad of beneficial actions.

One of the most evident results of Treg expansion has been the prevention of retinal thinning as a consequence of the preservation of retinal neurons (i.e. photoreceptors, bipolar cells, amacrine cells and RGCs). The other meaningful effect has been the abrogation of both macroglia and microglia activation and one of its main consequences: neuroinflammation. Although the vast majority of the detected $Iba1^+$ cells were microglia, the role of the remaining 8% in the development of DR has yet to be determined. Similar effects have already been reported in other CNS pathologies [13, 16, 17]. It should be noted that in the setting of DR, inflammation is as a key pathogenic factor that occurs before vascular changes can be detected [7–9] and as in many other neurodegenerative diseases, inflammasome activation is a well-stablished pathogenic mechanism [45] contributing to the heightened inflammatory response and the breakdown of the of the blood-retinal barrier (BRB) [35, 46, 47]. Our results have shown that Treg mitigate these effects by decreasing the retinal levels of NLRP3, IL-18 and Caspase-1, neutralizing at least one of the key innate-immune system driven inflammatory components and thus, facilitating the preservation of the neuroretina and the BRB.

Treg cells are able to mitigate vascular damage in chronic inflammatory conditions and in ocular diseases [25, 48]. In the retina, Treg have demonstrated the ability to repair vasculopathy in a model of oxygen-induced retinopathy [25]. Treg are recruited to the retina and, upon expansion, effectively reduced neovascularization, vascular leakage, and VEGF expression by altering the activation of microglia and inflammatory status [25]. We have broadened the understanding of Treg cells in mitigating vascular damage in retinal pathologies, as Treg expansion significantly decreased vascular tortuosity and leakage in the diabetic retina. This signifies a restoration of BRB function that was aligned to decrease in VEGF level, which were brought to levels observed in non-diabetic animals. Given that VEGF, besides a proinflammatory cytokine, is also a primary pathogenic mediator of vascular leakage [39], its normalization is an important mechanistic explanation supporting the vasculotropic effects of Treg expansion. The reason by which Treg prevented the diabetes-induced upregulation of VEGF within the retina could be associated with the concomitant decrease of inflammasome. In fact, proinflammatory cytokines are one of the most important triggers of VEGF production by the retina in situations in which the hypoxia, as is the case, is not predominant [49].

The role of Treg expansion in preventing retinal neurodegeneration in DR is evident in various retinal neural populations, including photoreceptors, bipolar cells, and retinal ganglion cells. We found significant retinal thinning in diabetic animals, which Treg expansion effectively prevented. Measurements of rod and cone density, amacrine cells, bipolar morphology, and retinal ganglion cell density were reduced in diabetic groups but restored by Treg expansion, highlighting its effect on DR-associated neurodegeneration. However, retinal neurodegeneration also involves inflammation, glial cell contributions and vascular damage that exacerbate the condition in db/db mice. Our study revealed significant changes in glial reactivity, inflammasome activation, and vascular leakage, all mitigated by Treg expansion. We cannot attribute the beneficial effects of Treg expansion to a single cell type or establish a precise sequence of events based

on our current data. Given the well-documented pleiotropic effects of Tregs across multiple cell types [13–15], the protective impact of Treg expansion in the DR retina likely results from their combined action across various retinal cells.

Current treatments for DR are only addressed to advanced stages of the disease when vision could already be compromised. These treatments include laser photocoagulation, intravitreal injections of corticosteroids or anti-angiogenic agents (i.e. VEGF) and vitreoretinal surgery. All of them present limited effectiveness and are associated with significant adverse effects [50]. At present, treatment of early stages of DR consists in controlling risk factors such hyperglycemia, hypertension and dyslipidemia, but there are no specific treatments to prevent or arrest the progression to advanced stages [51]. Topical (i.e. eye drops) drug formulations based on neuroprotective or anti-inflammatory agents capable of penetrating the retina have emerged as a new therapeutic approach for early stages of DR [52]. This route of administration could reduce systemic side effects and enable patients to self-administer treatment over extended periods. However, clinical evidence in terms of effectiveness and safety is scarce and specific trials are needed [53]. Therefore, the treatment of early stages of DR is an important unmet medical need. Our results have shown that endogenous Treg expansion prevents DR-associated neurodegeneration, inflammation and vascular leakage. In fact, Treg have demonstrated neuroprotective, pro-remyelinating, and immunomodulatory roles in various CNS diseases with pathophysiological features shared with DR [13, 54], and also in aged retinas [21]. Taken together, Treg expansion seems a promising therapeutic avenue for treating DR.

The present study has several limitations. First, we cannot assure that the beneficial effects can be exclusively due to retinal Treg expansion. However, the lack of changes in metabolic profile and diabetic milieu suggests that Treg expansion is primarily responsible for directly reducing inflammation and preventing neuronal and vascular damage associated with DR, instead of changing the overall metabolic profile. The second limitation of this study is the reliance on morphological analysis to infer visual function, which carries the risk of over-extrapolation. While morphological changes provide valuable insights, they do not directly correlate with functional outcomes. To address this, further experiments, such as electroretinography (ERG) and optokinetic assessments, are needed to evaluate visual function more comprehensively and validate the implications of our findings. The last limitation is that the induction of peripheral immunosuppression can be associated risk of infection, especially in patients with T2D. This is a serious problem to translate our findings to the clinical arena. However, new therapeutic strategies that increase Treg exclusively in damaged neural tissues, such as adeno-associated virus (AAV)-based delivery of IL-2, have proven effective in various experimental CNS-neuroinflammatory models [17, 18] and may open a new therapeutic avenue to build upon our findings.

## Conclusions

Treg expansion is a promising new therapeutic strategy to prevent the most important pathological features of DR: neurodegeneration, vascular leakage and glial cell activation. Future work is needed to explore methods to exploit Treg expansion exclusively in the eye to avoid potential systemic side effects and also to delve in the understanding of the intricated molecular mechanisms involved in Treg- mediated retinal protection in T2D.

### Abbreviations

| | |
|---|---|
| AAV | Adeno-Associated Virus |
| AD | Alzheimer's Disease |
| CA | Cone Arrestin |
| CD | Cognitive Decline |
| ChAT | Choline Acetyltransferase |
| CNS | Central Nervous System |
| DAPI | 4',6-diamidino-2-phenylindole |
| db/db | BKS.Cg-Dock7m +/+ Leprdb/J |
| DR | Diabetic Retinopathy |
| GCL | Ganglion Cell Layer |
| GFAP | Glial Fibrillary Acidic Protein |
| HbA1c | glycosylated haemoglobin A1 |
| HBSS | Hanks Buffered Salt Solution |
| IBA-1 | Ionized calcium binding adaptor molecule 1 |
| IL-2 | Interleukin-2 |
| INL | Inner-Nuclear Layer |
| i.p. | Intraperitoneal |
| IPL | Inner Plexiform Layer |
| mAb | Monoclonal Antibody |
| MS | Multiple Sclerosis |
| NVU | Retinal Neurovascular Unit |
| ONL | Outer-Nuclear Layer |
| PBS | Phosphate-Buffered Saline |
| PD | Parkinson's Disease |
| RBPMS | RNA-Binding Protein with Multiple Splicing |
| RGC | Retinal Ganglion Cells |
| T2D | Type 2 Diabetes mellitus |
| TH | Tyrosin Hidroxylase |
| Treg | Regulatory T cells |
| VEGF | Vascular endothelial growth factor |

## Supplementary Information

The online version contains supplementary material available at https://doi.org/10.1186/s12974-024-03323-0.

Supplementary Material 1

Supplementary Material 2

Supplementary Material 3

Supplementary Material 4

Supplementary Material 5

Supplementary Material 6

Supplementary Material 7

Supplementary Material 8

Supplementary Material 9

Supplementary Material 10

Supplementary Material 11

**Acknowledgements**
Special thanks to Professor Denise Fitzgerald and Prof. Adrian Liston for her useful advice on Treg biology. We also acknowledge extensive technical support from the staff of the Advance Technologies Unit at Vall d'Hebron Institut de Recerca, especially to Joan Puñet, Norberto Nuñez, Pilar Mancera, María Molinos and Cristina de Dios and Marta Valeri. We thank the staff of the animal facility at Vall d'Hebron for their assistance and animal maintenance.

**Author contributions**
Experiments were designed by M.L.S, M.T., A.G.F, A.W.S., C.H. and R.S. Experiments were performed by M.L.S, A.G.F, J.G.S., D.P.M-, A.D. M.G.R., A.D., A.A., P.B. and L.R. Experiments were analysed by M.L.S, M.T., A.G.F and D.P.M. Manuscript was written by M.L.S, A.G.F, C.H. and R.S. and with contributions from all authors. M.L.S. and R.S. oversaw the study.

**Funding**
This work has been partially supported by Col·legi Oficial de Farmacèutics de Barcelona. M.L.S.: Maria Zambrano fellowship from Spanish Ministry of Science, Innovation and Universities, financed by European Union "NextGenerationEU" (Universitat Autònoma de Barcelona), and Beatriu de Pinos fellowship, financed by Agència de Gestió d'Ajuts Universitaris i de Recerca (AGAUR, Generalitat de Catalunya). AGF research is supported by a Miguel Servet Fellowship from the Spanish Health Institute Carlos III (CP21/00032) and a grant from the Spanish State Research Agency corresponding to "Proyectos de Generación del Conocimiento 2021" (PID2021-124465OA-I00 funded by MICIU/AEI/13.13039/501100011033/ERDF, EU). JAGS research is supported by a Miguel Servet Fellowship from the Spanish Health Institute Carlos III (CP22/00078) and a grant from the Spanish State Research Agency corresponding to "Proyectos de Generación del Conocimiento 2022" (PID2022- 143269OB-I00).

**Data availability**
No datasets were generated or analysed during the current study.

## Declarations

**Ethics approval and consent to participate**
All animal experiments were directed in agreement with the European Community (86/609/CEE) and the guidelines of the Association for Research in Vision and Ophthalmology (ARVO) for the utilization of laboratory animals. The Animal Care and Use Committee of VHIR (CEEA 14/21) authorized the present study.

**Consent for publication**
N/A.

**Competing interests**
The authors declare no competing interests.

**Author details**
[1]Universitat Autònoma de Barcelona, Barcelona 08035, Spain
[2]Diabetes and Metabolism Research Unit, Vall d'Hebron Research Institute (VHIR), Barcelona, Spain
[3]Department of Psychiatry, Perelman School of Medicine, University of Pennsylvania, Philadelphia, PA, USA
[4]Ophthalmology Research Group, Vall d'Hebron Research Institut, Barcelona, Spain
[5]Centro de Investigación Biomédica en Red de Diabetes y Enfermedades Metabólicas Asociadas (CIBERDEM), Instituto de Salud Carlos III, Madrid, Spain
[6]Institute for Health and Biomedical Research of Alicante (ISABIAL), Alicante, Spain
[7]Institute of Neuroscience, CSIC-UMH, San Juan de Alicante, Spain
[8]Wellcome-Wolfson Institute for Experimental Medicine, Queen's University Belfast, Belfast, Northern Ireland BT9 7BL, UK

Received: 31 July 2024 / Accepted: 11 December 2024
Published online: 23 December 2024

**References**

1. Sun H, Saeedi P, Karuranga S, Pinkepank M, Ogurtsova K, Duncan BB, et al. IDF Diabetes Atlas: Global, regional and country-level diabetes prevalence estimates for 2021 and projections for 2045. Diabetes Res Clin Pract. 2022;183:109119. https://doi.org/10.1016/j.diabres.2021.109119.
2. Wong TY, Cheung CMG, Larsen M, Sharma S, Simó R. Diabetic retinopathy. Nat Rev Dis Primers. 2016;2:16012. https://doi.org/10.1038/nrdp.2016.12.
3. Bourne RRA, Steinmetz JD, Saylan M, Mersha AM, Weldemariam AH, Wondmeneh TG, et al. Causes of blindness and vision impairment in 2020 and trends over 30 years, and prevalence of avoidable blindness in relation to VISION 2020: The Right to Sight: An analysis for the Global Burden of Disease Study. Lancet Glob Health. 2021;9:e144–60. https://doi.org/10.1016/S2214-109X(20)30489-7.
4. Solomon SD, Chew E, Duh EJ, Sobrin L, Sun JK, VanderBeek BL, et al. Diabetic retinopathy: A position statement by the American Diabetes Association. Diabetes Care. 2017;40:412–8. https://doi.org/10.2337/dc16-2641.
5. Simó R, Stitt AW, Gardner TW. Neurodegeneration in diabetic retinopathy: does it really matter? Diabetologia. 2018;61:1902–12. https://doi.org/10.1007/s00125-018-4692-1.
6. Calle MC, Fernandez ML. Inflammation and type 2 diabetes. Diabetes Metab. 2012;38:183–91. https://doi.org/10.1016/j.diabet.2011.11.006.
7. Forrester JV, Kuffova L, Delibegovic M. The Role of Inflammation in Diabetic Retinopathy. Front Immunol. 2020;11:583687. https://doi.org/10.3389/fimmu.2020.583687.
8. Xue M, Mao X, Chen M, Yin W, Yuan S, Liu Q. The Role of Adaptive Immunity in Diabetic Retinopathy. J Clin Med. 2022;11. https://doi.org/10.3390/jcm11216499.
9. Yue T, Shi Y, Luo S, Weng J, Wu Y, Zheng X. The role of inflammation in immune system of diabetic retinopathy: Molecular mechanisms, pathogenetic role and therapeutic implications. Front Immunol. 2022;13. https://doi.org/10.3389/fimmu.2022.1055087.
10. Cantón A, Martinez EM. CD4-CD8 and CD28 expression in T Cells infiltrating the vitreous fluid in patients with proliferative diabetic retinopathy a flow cytometric analysis. 2004;122.
11. Llorián-Salvador M, Cabeza-Fernández S, Gomez-Sanchez JA, de la Fuente AG. Glial cell alterations in diabetes-induced neurodegeneration. Cell Mol Life Sci. 2024;81. https://doi.org/10.1007/s00018-023-05024-y.
12. Byrne EM, Llorián-Salvador M, Tang M, Margariti A, Chen M, Xu H. Il-17a damages the blood–retinal barrier through activating the janus kinase 1 pathway. Biomedicines 2021;9. https://doi.org/10.3390/biomedicines9070831
13. Evans FL, Dittmer M, de la Fuente AG, Fitzgerald DC. Protective and Regenerative Roles of T Cells in Central Nervous System Disorders. Front Immunol. 2019;10. https://doi.org/10.3389/fimmu.2019.02171.
14. Okeke EB, Uzonna JE. The pivotal role of regulatory T cells in the regulation of innate immune cells. Front Immunol. 2019;10. https://doi.org/10.3389/fimmu.2019.00680.
15. MacHhi J, Kevadiya BD, Muhammad IK, Herskovitz J, Olson KE, Mosley RL, et al. Harnessing regulatory T cell neuroprotective activities for treatment of neurodegenerative disorders. Mol Neurodegener. 2020;15. https://doi.org/10.1186/s13024-020-00375-7.
16. Dombrowski Y, O'Hagan T, Dittmer M, Penalva R, Mayoral SR, Bankhead P, et al. Regulatory T cells promote myelin regeneration in the central nervous system. Nat Neurosci. 2017;20:674–80. https://doi.org/10.1038/nn.4528.
17. Lemaitre P, Tareen SH, Pasciuto E, Mascali L, Martirosyan A, Callaerts-Vegh Z, et al. Molecular and cognitive signatures of ageing partially restored through synthetic delivery of IL2 to the brain. EMBO Mol Med. 2023;15. https://doi.org/10.15252/emmm.202216805.
18. Yshii L, Pasciuto E, Bielefeld P, Mascali L, Lemaitre P, Marino M, et al. Astrocyte-targeted gene delivery of interleukin 2 specifically increases brain-resident regulatory T cell numbers and protects against pathological neuroinflammation. Nat Immunol. 2022;23:878–91. https://doi.org/10.1038/s41590-022-01208-z.
19. Louapre C, Rosenzwajg M, Golse M, Roux A, Pitoiset F, Adda L, et al. A randomized double-blind placebo-controlled trial of low-dose interleukin-2 in

relapsing–remitting multiple sclerosis. J Neurol. 2023;270:4403–14. https://doi.org/10.1007/s00415-023-11690-6.
20. Webster KE, Walters S, Kohler RE, Mrkvan T, Boyman O, Surh CD, et al. In vivo expansion of t reg cells with il-2-mab complexes: induction of resistance to eae and long-term acceptance of islet allografts without immunosuppression. J Exp Med. 2009;206:751–60. https://doi.org/10.1084/jem.20082824.
21. Llorián-Salvador M, de Fuente AG, McMurran CE, Dashwood A, Dooley J, Liston A et al. Regulatory T cells limit age-associated retinal inflammation and neurodegeneration. Mol Neurodegener 2024;19. https://doi.org/10.1186/s13024-024-00724-w
22. Qiao YC, Shen J, He L, Hong XZ, Tian F, Pan YH et al. Changes of Regulatory T Cells and of Proinflammatory and Immunosuppressive Cytokines in Patients with Type 2 Diabetes Mellitus: A Systematic Review and Meta-Analysis. J Diabetes Res. 2016;2016. https://doi.org/10.1155/2016/3694957
23. Sheikh V, Zamani A, Mahabadi-Ashtiyani E, Tarokhian H, Borzouei S, Alahgholi-Hajibehzad M. Decreased regulatory function of CD4 + CD25 + CD45RA + T cells and impaired IL-2 signalling pathway in patients with type 2 diabetes mellitus. Scand J Immunol. 2018;88. https://doi.org/10.1111/sji.12711.
24. Wang M, Chen F, Wang J, Zeng Z, Yang Q, Shao S. Th17 and Treg lymphocytes in obesity and Type 2 diabetic patients. Clin Immunol. 2018;197:77–85. https://doi.org/10.1016/j.clim.2018.09.005.
25. Deliyanti D, Talia DM, Zhu T, Maxwell MJ, Agrotis A, Jerome JR, et al. Foxp3 + Tregs are recruited to the retina to repair pathological angiogenesis. Nat Commun. 2017;8:1–12. https://doi.org/10.1038/s41467-017-00751-w.
26. Bogdanov P, Corraliza L, Villena A, Carvalho J, Garcia-Arumí AR, Ramos J. The db/db Mouse: A Useful Model for the Study of Diabetic Retinal Neurodegeneration. PLoS ONE. 2014;9:e97302.
27. Ren J, Zhang S, Pan Y, Jin M, Li J, Luo Y, et al. Diabetic retinopathy: Involved cells, biomarkers, and treatments. Front Pharmacol. 2022;13. https://doi.org/10.3389/fphar.2022.953691.
28. Cuenca N, Fernández-Sánchez L, Campello L, Maneu V, De la Villa P, Lax P, et al. Cellular responses following retinal injuries and therapeutic approaches for neurodegenerative diseases. Prog Retin Eye Res. 2014;43:17–75. https://doi.org/10.1016/j.preteyeres.2014.07.001.
29. Liu F, Saul AB, Pichavaram P, Xu Z, Rudraraju M, Somanath PR, et al. Pharmacological inhibition of spermine oxidase reduces neurodegeneration and improves retinal function in diabetic mice. J Clin Med. 2020;9. https://doi.org/10.3390/jcm9020340.
30. Gastinger MJ, Singh RSJ, Barber AJ. Loss of Cholinergic and Dopaminergic Amacrine Cells in Streptozotocin-Diabetic Rat and Ins2 $^{Akita}$ -Diabetic Mouse Retinas. Invest Opthalmology Visual Sci. 2006;47:3143. https://doi.org/10.1167/iovs.05-1376.
31. Ma M, Xu Y, Xiong S, Zhang J, Gu Q, Ke B, et al. Involvement of ciliary neurotrophic factor in early diabetic retinal neuropathy in streptozotocin-induced diabetic rats. Eye. 2018;32:1463–71. https://doi.org/10.1038/s41433-018-0110-7.
32. Altmann C, Schmidt MHH. The role of microglia in diabetic retinopathy: Inflammation, microvasculature defects and neurodegeneration. Int J Mol Sci. 2018;19. https://doi.org/10.3390/ijms19010110.
33. Coughlin BA, Feenstra DJMS. Müller Cells and Diabetic Retinopathy. Vis Res. 2017;139:93–100. https://doi.org/10.1016/j.visres.2017.03.013.
34. Voet S, Srinivasan S, Lamkanfi M, van Loo G. Inflammasomes in neuroinflammatory and neurodegenerative diseases. EMBO Mol Med. 2019;11. https://doi.org/10.15252/emmm.201810248.
35. Zheng X, Wan J, Tan G. The mechanisms of NLRP3 inflammasome/pyroptosis activation and their role in diabetic retinopathy. Front Immunol. 2023;14. https://doi.org/10.3389/fimmu.2023.1151185.
36. McCurry CM, Sunilkumar S, Subrahmanian SM, Yerlikaya EI, Toro AL, VanCleave AM, et al. NLRP3 Inflammasome Priming in the Retina of Diabetic Mice Requires REDD1-Dependent Activation of GSK3β. Invest Ophthalmol Vis Sci. 2024;65. https://doi.org/10.1167/iovs.65.3.34.
37. Sasongko MB, Wong TY, Nguyen TT, Cheung CY, Shaw JE, Wang JJ. Retinal vascular tortuosity in persons with diabetes and diabetic retinopathy. Diabetologia. 2011;54:2409–16. https://doi.org/10.1007/s00125-011-2200-y.
38. Simó R, Bogdanov P, Ramos H, Huerta J, Simó-Servat O, Hernández C. Effects of the topical administration of semaglutide on retinal neuroinflammation and vascular leakage in experimental diabetes. Biomedicines. 2021;9. https://doi.org/10.3390/biomedicines9080926.
39. Gupta N, Mansoor S, Sharma A, Sapkal A, Sheth J, Falatoonzadeh P et al. Diabetic Retinopathy and VEGF. 2013;7.
40. Burke SJ, Batdorf HM, Burk DH, Noland RC, Eder AE, Boulos MS, et al. Db / db Mice Exhibit Features of Human Type 2 Diabetes That Are Not Present in Weight-Matched C57BL/6J Mice Fed a Western Diet. J Diabetes Res. 2017;2017. https://doi.org/10.1155/2017/8503754.
41. Sheikh V, Zamani A, Mahabadi-Ashtiyani E, Tarokhian H, Borzouei S, Alahgholi-Hajibehzad M. Decreased regulatory function of CD4 + CD25 + CD45RA + T cells and impaired IL-2 signalling pathway in patients with type 2 diabetes mellitus. Scand J Immunol. 2018;88. https://doi.org/10.1111/sji.12711.
42. Xu Q, Zhang X, Li T, Shao S. Exenatide regulates Th17/Treg balance via PI3K/Akt/FoxO1 pathway in db/db mice. Mol Med. 2022;28:144. https://doi.org/10.1186/s10020-022-00574-6.
43. Wang D, Zhang Q, Dong W, Ren S, Wang X, Su C, et al. SGLT2 knockdown restores the Th17/Treg balance and suppresses diabetic nephropathy in db/db mice by regulating SGK1 via Na+. Mol Cell Endocrinol. 2024;584:112156. https://doi.org/10.1016/j.mce.2024.112156.
44. Eller K, Kirsch A, Wolf AM, Sopper S, Tagwerker A, Stanzl U, et al. Potential role of regulatory T cells in reversing obesity-linked insulin resistance and diabetic nephropathy. Diabetes. 2011;60:2954–62. https://doi.org/10.2337/db11-0358.
45. Piancone F, La Rosa F, Marventano I, Saresella M, Clerici M. The role of the inflammasome in neurodegenerative diseases. Molecules 2021;26. https://doi.org/10.3390/molecules26040953
46. Chaurasia SS, Lim RR, Parikh BH, Wey YS, Tun BB, Wong TY, et al. The NLRP3 Inflammasome May Contribute to Pathologic Neovascularization in the Advanced Stages of Diabetic Retinopathy. Sci Rep. 2018;8. https://doi.org/10.1038/s41598-018-21198-z.
47. Loukovaara S, Piippo N, Kinnunen K, Hytti M, Kaarniranta K, Kauppinen A. NLRP3 inflammasome activation is associated with proliferative diabetic retinopathy. Acta Ophthalmol. 2017;95:803–8. https://doi.org/10.1111/aos.13427.
48. Lužnik Z, Anchouche S, Dana R, Yin J. Regulatory T Cells in Angiogenesis. J Immunol. 2020;205:2557–65. https://doi.org/10.4049/jimmunol.2000574.
49. Simó R, Sundstrom JM, Antonetti DA. Ocular anti-VEGF therapy for diabetic retinopathy: The role of VEGF in the pathogenesis of diabetic retinopathy. Diabetes Care. 2014;37:893–9. https://doi.org/10.2337/dc13-2002.
50. Simó R, Hernández C. New Insights into Treating Early and Advanced Stage Diabetic Retinopathy. Int J Mol Sci. 2022;23. https://doi.org/10.3390/ijms23158513.
51. Simó R, Hernández C. What else can we do to prevent diabetic retinopathy? Diabetologia. 2023;66:1614–21. https://doi.org/10.1007/s00125-023-05940-5.
52. Simó R, Simó-Servat O, Bogdanov P, Hernández C. Neurovascular unit: A new target for treating early stages of diabetic retinopathy. Pharmaceutics. 2021;13. https://doi.org/10.3390/pharmaceutics13081320.
53. Thagaard MS, Vergmann AS, Grauslund J. Topical treatment of diabetic retinopathy: a systematic review. Acta Ophthalmol. 2022;100:136–47. https://doi.org/10.1111/aos.14912.
54. de la Fuente AG, Dittmer M, Heesbeen EJ, de la Vega Gallardo N, White JA, Young A, et al. Ageing impairs the regenerative capacity of regulatory T cells in mouse central nervous system remyelination. Nat Commun. 2024;15. https://doi.org/10.1038/s41467-024-45742-w.

## Publisher's note